International Journal of Civil and Structural Engineering Research ISSN 2348-7607 (Online)
Vol. 6, Issue 1, pp: (267-281), Month: April - September 2018, Available at: www.researchpublish.com

FINITE ELEMENT MODELING OF CONCRETE SOLID SLABS REINFORCED USING G.F.R.P. REBAR

[1]Nasr Z. Hassan, [2]Mirhan W. Adly

[1]Assoc. Prof. of Concrete Structures, Faculty of Eng., Mattaria, Helwan Univ., Cairo, Egypt
[2]Teaching Assistant, Construction Engineering Dept., Egyptian Russian University, Cairo, Egypt

Abstract: **Concrete structures that deteriorate throughout the world have become a major problem, so the cost of repair and rehabilitation due to these deteriorate has become a major concern to engineers and researchers. One of the preferable solutions of repair is to use fiber reinforced polymer (FRP) rebar in concrete. Although there are many researchers who covered different subjects of concrete reinforced with GFRP-bars, there are few researchers which are concerned with concrete solid plates reinforced using GFRP-bars. FRP is a composite made of reinforcement imbedded in a plastic (polymer) matrix. Physical and mechanical properties of FRP depend mainly on the type of fibers and resins used to form the composite. Such differences arise from the interaction mechanism between FRP reinforcement bars and concrete element. Although there are many researchers who covered different subjects of concrete slabs reinforced with GFRP-bars, there are few researchers which are concerned with concrete slabs which are reinforced with GFRP-bars.In this study a finite element program executed on seventy solid slabs specimen reinforced by steel and GFRP rebar (one way and two way slabs) with different rectangularity ratio, this research studies the flexure behavior of slabs through the following parameters:**

a- Type of load as single line load, two lines load and uniform loads.

b- Types of reinforcement rebar as steel and GFRP rebar.

c- Rectangularity ratio of slab as one way and two way slabs

d- Reinforcement ratio.

Keywords: **Solid plates, Flexure strength, GFRP rebar, Crack pattern.**

1. INTRODUCTION

The need to replace the steel as a material with large ability for corrosion by recent composite materials reinforcing material for concrete element subjected to aggressive environments became essential due to rise of cost of maintenance for these structures and also in countries where steel became a very expensive material to be either produced or used.

Researchers in the last four decays were aware of the difficulties of using fiber polymers [1] as reinforcements due to its defects such as its lower elastic modulus compared to steel, its brittleness (lack of ductility), and the weak bond strength with concrete [2], [3]. The researchers in this field continued on a lower level through the seventies of the last century.

The practical use of this composite material [4], [5] began approximately at the beginning of eighties. Also the need of electromagnetically neutral materials to replace steel as concrete reinforcement became necessary in specific applications because of the interfered steel with sensitive equipment of the operation. Composite material like glass and carbon fiber become center of attention in the field of structural engineering due to their excellent properties such as non-corrosive, nonconductive and nonmagnetic properties to overcome the corrosion problem in bridge decks, parking garages, water and wastewater treatment facilities, marine structures and chemicals plants. This study focuses on Glass Fiber Reinforced Polymer GFRP [6], [7] reinforced concrete one way slabs performance under loads [8], [9], [10], [11].

2. PROGRAM STUDY

The analyzed slab specimens which shown in Table (1) were carried out on seventy solid slab specimens (one way and two way slabs) with different rectangularity ratio. The specimen divided into ten groups, each group have seven specimens the first specimen reinforced using steel reinforcement, As the other six specimens reinforced using GFRB rebar with different reinforcement ration ranging from 0.55 % to 1.3 %. The applied load taken as, one line load in short direction as shown in Figure(1), two lines loads in short direction in Figure (2), two orthogonal lines loads Figure(3) and uniform load Figure(4). Groups 1, 2 and 7 are one way slabs, of 1600 mm long, 500 mm width and 100 mm depth, groups 3, 4 and 8 are two way slabs of rectangularity ratio equal 2 with dimensions 1000 mm long, 500 mm width and 100 mm depth, groups 5 and 9 are two way slabs of rectangularity ratio equal 1.5 with dimensions 1500 mm long, 1000 mm wide and 100 mm depth, while groups 6 and 10 are two way slabs of rectangularity ratio equal 1.0 with dimensions 1000 mm long, 1000 mm width and 100 mm depth.

TABLE (1): Specimen Details

Group	Slab No.	Reinforcement	Material	Dimensions (mm) (Rectangularity ratio)	Type of Loads	Type of Slabs	μ %
1	S-1-1	6 Ø 10/m'	Steel	1600*500*100 (3.2)	One line load in short direction	One way slab	0.55
	S-1-2	6 Ø 10/m'	GFRP				0.55
	S-1-3	8 Ø 10/m'					0.73
	S-1-4	10 Ø 10/m'					0.92
	S-1-5	6 Ø 12/m'					0.797
	S-1-6	8 Ø 12/m'					1.06
	S-1-7	10 Ø 12/m'					1.30
2	S-2-1	6 Ø 10/m'	Steel	1600*500*100 (3.2)	Two lines load in short direction	One way slab	0.55
	S-2-2	6 Ø 10/m'	GFRP				0.55
	S-2-3	8 Ø 10/m'					0.73
	S-2-4	10 Ø 10/m'					0.92
	S-2-5	6 Ø 12/m'					0.797
	S-2-6	8 Ø 12/m'					1.06
	S-2-7	10 Ø 12/m'					1.30
3	S-3-1	6 Ø 10/m'	Steel	1000*500*100 (2.0)	One line load in short direction	Two way slab	0.55
	S-3-2	6 Ø 10/m'	GFRP				0.55
	S-3-3	8 Ø 10/m'					0.73
	S-3-4	10 Ø 10/m'					0.92
	S-3-5	6 Ø 12/m'					0.797
	S-3-6	8 Ø 12/m'					1.06
	S-3-7	10 Ø 12/m'					1.30
4	S-4-1	6 Ø 10/m'	Steel	1000*500*100 (2.0)	Two lines load in short direction	Two way slab	0.55
	S-4-2	6 Ø 10/m'	GFRP				0.55
	S-4-3	8 Ø 10/m'					0.73
	S-4-4	10 Ø 10/m'					0.92
	S-4-5	6 Ø 12/m'					0.797
	S-4-6	8 Ø 12/m'					1.06
	S-4-7	10 Ø 12/m'					1.30
5	S-5-1	6 Ø 10/m'	Steel	1500*1000*100 (1.5)	Two orthogonal lines load	Two way slab	0.55
	S-5-2	6 Ø 10/m'	GFRP				0.55
	S-5-3	8 Ø 10/m'					0.73
	S-5-4	10 Ø 10/m'					0.92
	S-5-5	6 Ø 12/m'					0.797
	S-5-6	8 Ø 12/m'					1.06
	S-5-7	10 Ø 12/m'					1.30

Group	Slab No.	Reinforcement	Material	Dimensions (mm)	Type of Loads	Type of Slabs	μ %
6	S-6-1	6 Ø 10/m'	Steel	1000*1000*100 (1.0)	Two orthogonal lines load	Two way slab	0.55
	S-6-2	6 Ø 10/m'	GFRP				0.55
	S-6-3	8 Ø 10/m'					0.73
	S-6-4	10 Ø 10/m'					0.92
	S-6-5	6 Ø 12/m'					0.797
	S-6-6	8 Ø 12/m'					1.06
	S-6-7	10 Ø 12/m'					1.30
7	S-7-1	6 Ø 10/m'	Steel	1600*500*100 (3.2)	Uniform load	One way slab	0.55
	S-7-2	6 Ø 10/m'	GFRP				0.55
	S-7-3	8 Ø 10/m'					0.73
	S-7-4	10 Ø 10/m'					0.92
	S-7-5	6 Ø 12/m'					0.797
	S-7-6	8 Ø 12/m'					1.06
	S-7-7	10 Ø 12/m'					1.30
8	S-8-1	6 Ø 10/m'	Steel	1000*500*100 (2.0)	Uniform load	Two way slab	0.55
	S-8-2	6 Ø 10/m'	GFRP				0.55
	S-8-3	8 Ø 10/m'					0.73
	S-8-4	10 Ø 10/m'					0.92
	S-8-5	6 Ø 12/m'					0.797
	S-8-6	8 Ø 12/m'					1.06
	S-8-7	10 Ø 12/m'					1.30
9	S-9-1	6 Ø 10/m'	Steel	1500*1000*100 (1.5)	Uniform load	Two way slab	0.55
	S-9-2	6 Ø 10/m'	GFRP				0.55
	S-9-3	8 Ø 10/m'					0.73
	S-9-4	10 Ø 10/m'					0.92
	S-9-5	6 Ø 12/m'					0.797
	S-9-6	8 Ø 12/m'					1.06
	S-9-7	10 Ø 12/m'					1.30
10	S-10-1	6 Ø 10/m'	Steel	1000*1000*100 (1.0)	Uniform load	Two way slab	0.55
	S-10-2	6 Ø 10/m'	GFRP				0.55
	S-10-3	8 Ø 10/m'					0.73
	S-10-4	10 Ø 10/m'					0.92
	S-10-5	6 Ø 12/m'					0.797
	S-10-6	8 Ø 12/m'					1.06
	S-10-7	10 Ø 12/m'					1.30

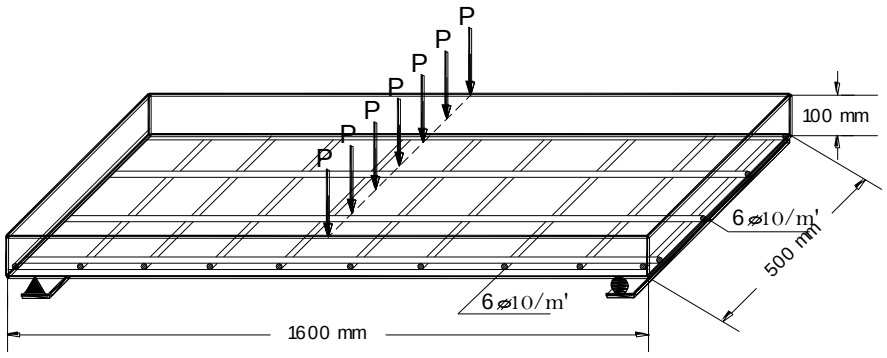

Fig 1: One line load in short direction (groups 1 and 3)

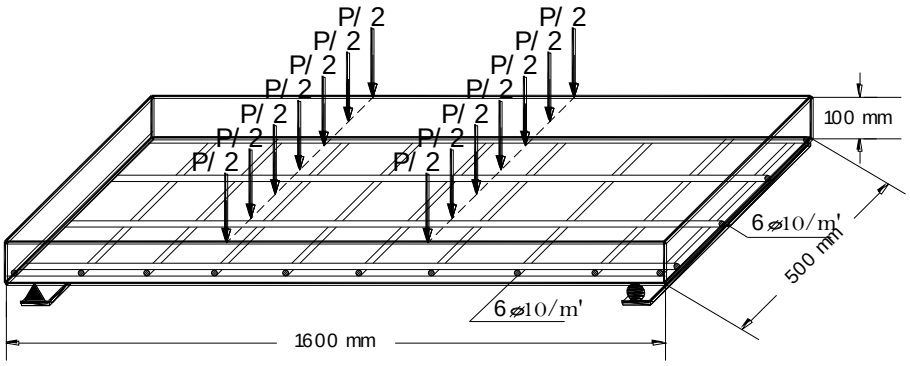

Fig 2: Two lines load in short direction (groups 2 and 4)

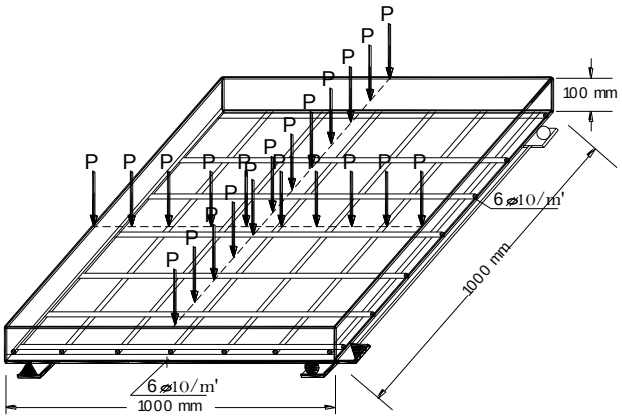

Fig 3: Two orthogonal lines load (groups 5 and 6)

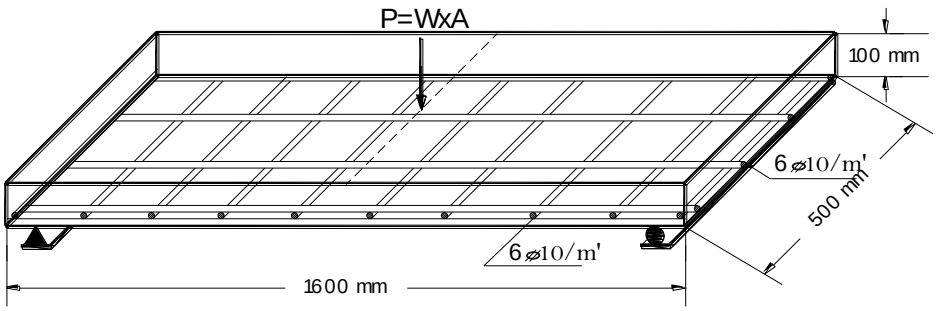

Fig 4: Uniform loads (groups 7, 8, 9 and 10)

2.1 Verification of Finite Element Results:

Verification is carried out to check the validity and accuracy of results of finite element program. The accuracy of the finite element models is specified by making sure that failure modes are same and the failure load value is reasonably predicted to same as compared with the experimental results, according to Haggag [12], [13]. Seven specimens of one way slab are modeled. The finite element analysis results will be compared with that to the experimental results in the Table (2).

Haggag [12], [13] prepared an experimental study by using seven slabs specimens are tested to assess the influence of using GFRP bars in addition to steel reinforcement. These specimens used as verification group as group 2 listed in the program study to verify the output of ANSYS [14] modeling.

Table (2) represents both the experimental results compared to which of finite element study at cracking stage and failure stage. It is noted by comparing the results the tolerance between experimental results of failure load and finite element study values was within 4 % except for specimen S-2-4 it was about 18 % difference.

TABLE (2): FEM Results versus Experimental Results for Verification Specimens (Group 2)

Group	Slab No.	Cracking Stage		Failure Stage		Ultimate Stage from ACI&ECP208 P_u (kN)	$P_{Exp.}$ / P_{FEM} (%)
		Exp.	FEM	Exp.	FEM		
		P_{cr} (kN)	P_{cr} (kN)	P_f (kN)	P_f (kN)		
2	S-2-1	17	15.5	22	21	29.0	104.7
	S-2-2	8.6	9.2	25	24.6	25.0	101.6
	S-2-3	9.1	8.4	40	39.9	32.5	100.25
	S-2-4	9.9	13.8	40	33.9	41.5	117.99
	S-2-5	10	13.8	42	40	36.0	105
	S-2-6	10.9	10.9	48	47.32	47.0	96.38
	S-2-7	11.6	11.9	66	65	57.5	101.5

2.2 Numerical Analysis:

A nonlinear three dimensional brick element solid element, SOLID 65, is used to model the concrete in ANSYS program [14]. The solid element has eight nodes with three transitional degrees of freedom at each node. In addition, the element is capable of simulating plastic deformation, cracking in three orthogonal directions, and crushing.

in compression and creep.

Modeling of cracks through an adjustment of the material properties is done by changing the value of element stiffness matrices. If the concrete at an integration points fails in uniaxial, biaxial, or tri-axial compression, the concrete is assumed crushed at that point. Crushing is defined as the complete deterioration of the structural integrity of the concrete.

The element model of concrete is defined as eight nodes element having three degrees of freedom at each node Figure(5): translations in the nodal x, y, and z directions.

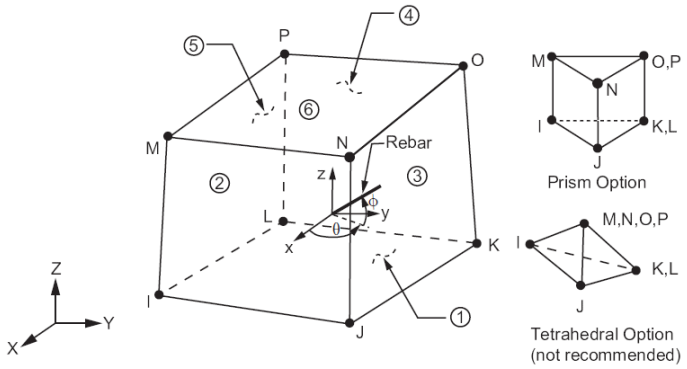

Fig 5: Solid65 element for concrete model

The longitudinal steel reinforcement is defined by a discrete axial element (LINK180) in ANSYS Program [14]. This element is a uniaxial tension-compression element with three translation degrees of freedom at each node Figure (6),modeling of steel bearing plate is Solid 45.

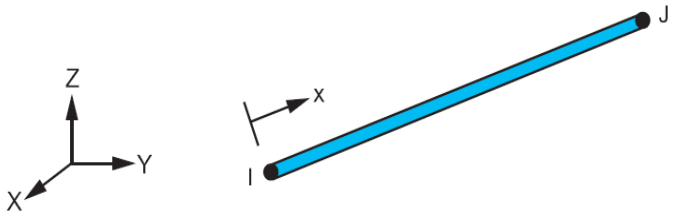

Fig 6: LINK180 geometry ANSYS R14.5 [14]

2.3 Modeling And Meshing:

Slabs specimens, plates, and supports modeled as volume, all models have a rectangular mesh of (25 mm x 25 mm). Figure(7) shows the meshing of specimens of all groups.

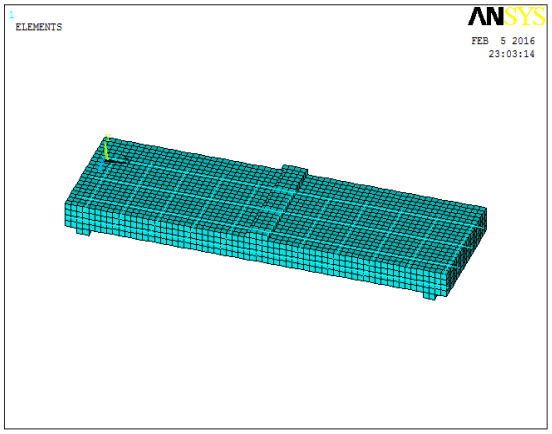

Groups 1 and 3

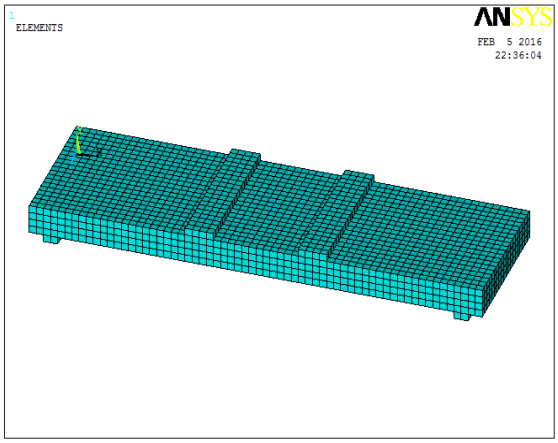

Groups 2 and 4

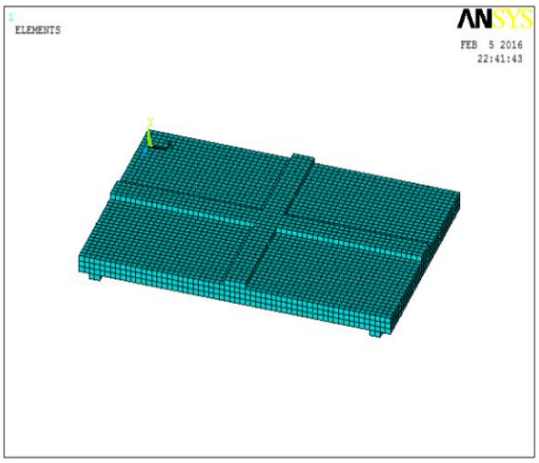

Groups 5 and 6

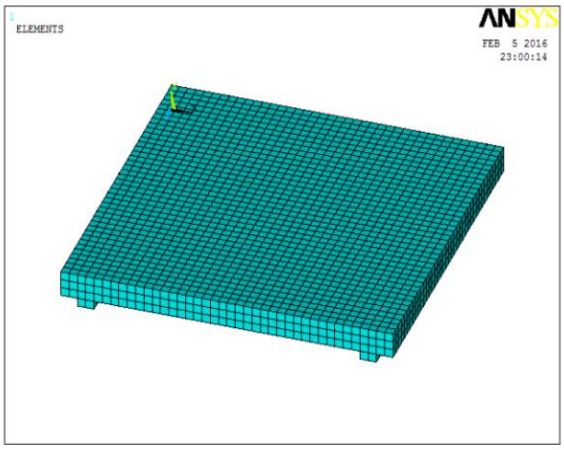

Groups 7, 8, 9 and 10

Fig 7: Modeling and meshing

3. THEORETICAL RESULTS

In the following, the results of the specimen behavior are discussed through Table (3). The values indicate central deflection and load values at both of cracking and failure stages for all specimens. The measurement of the ductility as ductility index represented as the ratio of deflection value at failure to that at cracking stage (μ_d) = Δ_f / Δ_{cr}, and absorbed energy calculated by area under the load-deflection curve, also cracking and failure load are listed in the same Table (3). The mode of failure for each specimen is finally determined according to the final cracked shapes before failure [15].

In group (1), all specimens of same dimensions 1600*500*100 mm, case of loading but different reinforcement ratio, failed in a typical tension mode The slab (S-1-1) was reinforced with steel bars. Specimens (S-1-2, S-1-3, S-1-4, S-1-5, S-1-6 and S-1-7) were reinforced with GFRP bars. From Table (3) we can see that, Slab (S-1-2 with μ= 0.55%) which reinforced with GFRP increased in the ductility index (μ_d) and the absorbed energy relative to the slab (S-1-1) have same dimensions and reinforcement ratio but reinforced with steel bars, this is due to the ductility property of GFRP bars which is more than steel bars.

In addition, the measure of ductility in most specimens was enhanced by using high reinforcement compared by control specimen, this reason is due to increasing surface area of GFRP bars (Ø12), minimum distance between bars and increasing the bond strength [16], [17] between GFRP bars and concrete. Reinforcement ratio effective and GFRP bars for all slabs (same type) have nearly the same effect.

TABLE (3): FEM Results

Group	Slab No.	Cracking Stage		Failure Stage		Ultimate stage from ACI & ECP-208 P_u (kN)	Ductility Index μd	Absorbed Energy kN.mm
		P_{equ} kN	Δ_{cr} mm	P_{equ} kN	Δ_f mm			
1	S-1-1	11.5	0.74	20.15	13.0	29.0	17.56	236.10
	S-1-2	14.6	0.59	24.30	15.0	25.0	25.42	239.24
	S-1-3	18.3	0.59	32.15	31.3	32.5	53.05	958.47
	S-1-4	8.0	0.37	33.20	13.7	41.5	37.02	853.64
	S-1-5	25	0.34	30.26	14.0	36.0	41.17	417.24
	S-1-6	23.7	0.59	46.6	31.5	47.0	53.38	1260.56
	S-1-7	30	0.45	60.3	31.0	57.5	68.88	1673.19
3	S-3-1	23.6	2.0	32.0	11.9	29.0	5.93	331.34
	S-3-2	18.3	2.35	33.5	15.8	40.0	6.72	412.75
	S-3-3	17.8	2.30	36.2	11.2	52.0	4.88	362.06
	S-3-4	14.6	2.25	48.0	9.99	66.4	4.44	350.03
	S-3-5	18.9	2.35	32.4	15.9	57.6	6.74	371.43
	S-3-6	21.9	2.35	52.0	19.0	75.2	8.09	724.33
	S-3-7	22.8	2.35	68.0	23.2	92.0	9.87	1221.29
4	S-4-1	24.6	1.90	38.7	7.50	43.0	3.95	245.11
	S-4-2	20.0	2.20	35.0	10.7	60.0	4.85	337.70
	S-4-3	7.80	2.10	38.9	18.6	78.0	8.86	486.82
	S-4-4	9.60	2.0	50.0	14.5	99.6	7.27	461.27
	S-4-5	20.0	2.20	35.0	4.85	86.4	2.20	148.65
	S-4-6	14.6	1.90	53.0	11.2	112.8	5.91	466.56
	S-4-7	13.3	2.10	70.0	10.5	138	5.00	441.04
5	S-5-1	10.8	1.19	19.8	16.2	29.0	13.62	234.03
	S-5-2	18.3	2.68	40.0	20.6	26.7	7.69	644.64
	S-5-3	12.0	2.60	45.6	12.1	34.6	4.66	365.46
	S-5-4	14.0	5.40	79.9	20.7	44.3	3.82	422.88
	S-5-5	17.3	1.18	57.8	14.0	38.4	11.86	572.71
	S-5-6	36.5	2.68	77.2	14.2	50.0	5.28	767.58
	S-5-7	25.3	1.19	87.7	18.4	61.3	15.48	1217.99

Group	Slab No.	Cracking Stage		Failure Stage		Ultimate stage from ACI & ECP-208 P_u (kN)	Ductility Index μd	Absorbed Energy kN.mm
		P_{equ} kN	Δ_{cr} mm	P_{equ} kN	Δ_f mm			
6	S-6-1	12.5	0.22	30.00	15.13	29.0	68.79	291.82
	S-6-2	10.5	0.33	44.13	19.28	40.0	58.42	527.50
	S-6-3	12.0	0.17	54.70	5.99	52.0	35.24	273.95
	S-6-4	14.0	0.74	96.50	7.00	66.4	9.46	408.31
	S-6-5	11.5	0.77	68.25	12.44	57.6	16.16	520.65
	S-6-6	28.3	3.06	88.25	19.20	75.2	6.27	1049.32
	S-6-7	33.9	3.10	93.90	15.65	92.0	5.05	906.25
7	S-7-1	8.70	6.90	33.12	28.60	57.5	4.14	740.11
	S-7-2	2.00	6.50	56.00	29.30	50.0	4.51	1476.76
	S-7-3	2.00	6.50	43.20	12.50	65.0	1.92	462.88
	S-7-4	1.60	6.00	43.36	12.53	83.0	2.09	462.88
	S-7-5	10.8	5.90	42.50	10.98	72.0	1.86	382.34
	S-7-6	2.00	5.40	48.00	6.10	94.0	1.13	268.16
	S-7-7	2.20	5.90	71.20	11.10	115	1.88	580.80
8	S-8-1	1.80	3.80	42.23	19.10	57.5	5.03	550.56
	S-8-2	1.15	2.25	48.00	21.00	80.0	9.33	827.33
	S-8-3	16.7	2.28	49.00	12.10	104	5.31	447.92
	S-8-4	15.7	2.75	50.00	16.80	132.8	6.11	699.00
	S-8-5	1.83	2.90	48.00	14.40	115.2	4.97	587.56
	S-8-6	11.3	2.60	55.00	16.73	150.4	6.43	675.26
	S-8-7	10.3	3.10	72.10	16.40	184	5.29	920.00

9	S-9-1	19.0	2.01	27.16	18.90	57.5	9.40	374.45
	S-9-2	16.0	1.23	44.55	22.35	53.3	18.17	865.89
	S-9-3	22.0	1.10	51.30	18.50	69.0	16.82	798.49
	S-9-4	21.0	6.75	82.30	25.20	88.5	3.73	1575.02
	S-9-5	9.00	1.23	59.30	31.00	76.8	25.20	1363.41
	S-9-6	12.0	4.36	79.25	29.30	100.3	6.72	1942.80
	S-9-7	12.0	1.23	89.20	16.96	122.6	13.79	1359.65
10	S-10-1	14.0	0.49	32.20	27.20	57.5	55.51	696.07
	S-10-2	10.0	1.46	47.10	27.10	80.0	18.56	983.34
	S-10-3	12.0	1.46	58.00	18.20	104	12.47	841.28
	S-10-4	13.2	3.94	98.0	27.20	132.8	6.90	2328.74
	S-10-5	5.40	0.49	71.30	24.15	115.2	49.29	1490.16
	S-10-6	11.2	1.48	98.50	21.16	150.4	14.30	1916.57
	S-10-7	14.0	3.60	100.0	16.81	184	4.67	1537.49

3.1 Load-Deflection Relationship:

Figure (8) to Figure (14) show the load to deflection relationship plotted from the finite element analyses for each slab in group (1) only at the last converged load step.

The load-deflection curves for all slabs (same type) have nearly the same shapes, where the load–deflection behavior of concrete elements typically includes three stages. Stage I: manifests the linear behavior of un-cracked elastic section, Stage II: implies initiation of concrete cracking and Stage III: relies relatively on steel reinforcements yielding and concrete crushing. In nonlinear iterative algorithms, ANSYS 14.5 [14] utilizes Newton–Raphson method [18], [19] for the incremental load analysis.

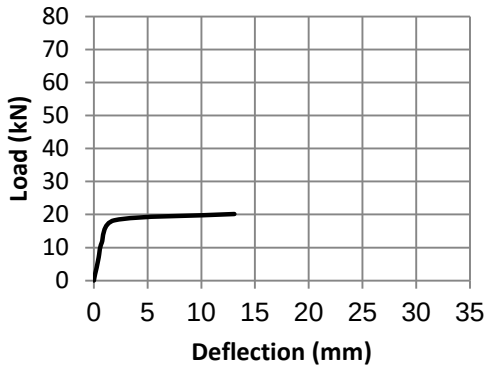

Fig 8: Load deflection curve (S-1-1)

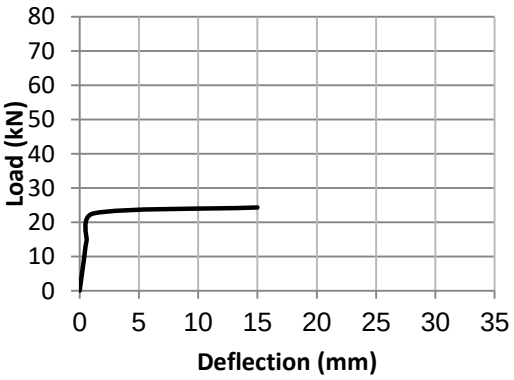

Fig 9: Load deflection curve (S-1-2)

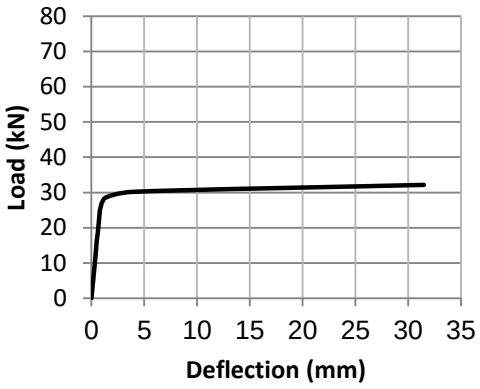

Fig 10: Load deflection curve (S-1-3)

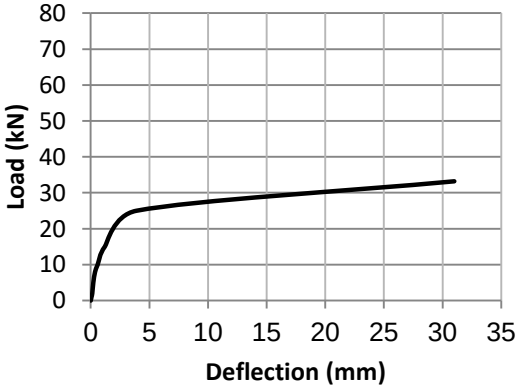

Fig 11: Load deflection curve (S-1-4)

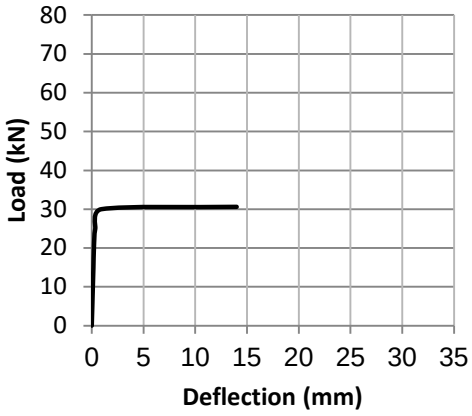

Fig 12: Load deflection curve (S-1-5)

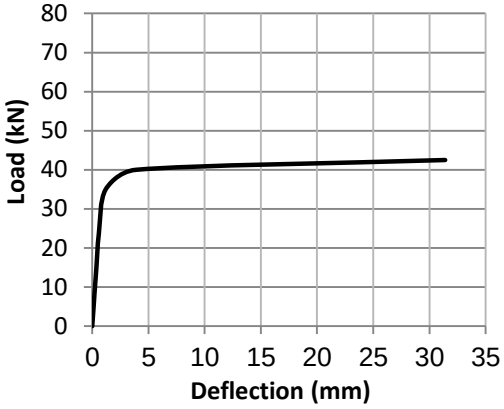

Fig 13: Load deflection curve (S-1-6)

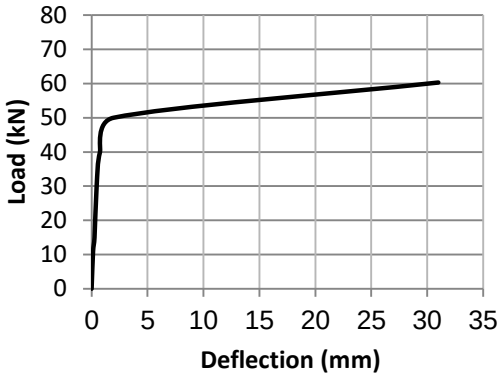

Fig 14: Load deflection curve (S-1-7)

Slabs has almost the same profile of the load deflection curves for where the first part of the curves are steep, and after cracking, most of the profiles start to be more curved until the failure occurs.

The measured values of the deflection at the mid-span of the bottom surface of the investigated slab and plotted versus the applied load from loading starting to failure.

The process of crack formation can be classified into three stages. The un-cracked stage is before the limiting tensile strength is reached, the crack formation occurs in the process zone of a potential crack with lessening tensile stress on crack face due to crack bridging effect and finally, after a complete release of the stress, the crack opening continues without the stress. The concrete tension failure is characterized by a piecemeal growth of cracks, which connect together and eventually disconnect larger parts of the structure.

Cracking is represented in the ANSYS program by a circle outline in the plane of the crack, while the crushing is shown with an octahedron outline. The first crack is shown with a red circle outline at integration point, the second crack with a green outline, the third crack with a blue outline and closed cracks are shown as X inside the circle which shown in Figure (15).

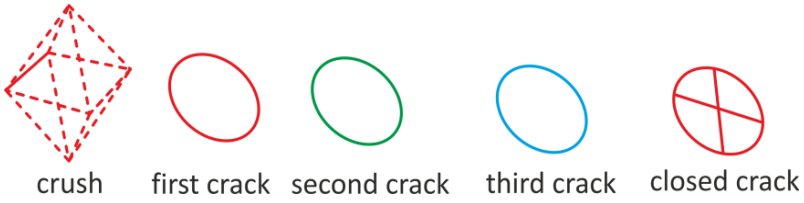

Fig 15: Symbols used by ANSYS to represent cracking and crushing,

ANSYS (SAS 2012)

Figure (16) shows evolutions of crack patterns obtained from ANSYS program [14] analyses for (S-1-1) to (S-1-7) in (group (1).

The first crack was a small longitudinal crack observed in a short direction in tension side at mid span of slab, and was accompanied by an increase in deflection due to stiffness reduction of the specimen. With increasing load many cracks are developed on the bottom of the slab. The behavior of models will be discussed to illustrate the effect of each of increasing reinforcement ratio in different slabs, loading type and rectangularity ratio.

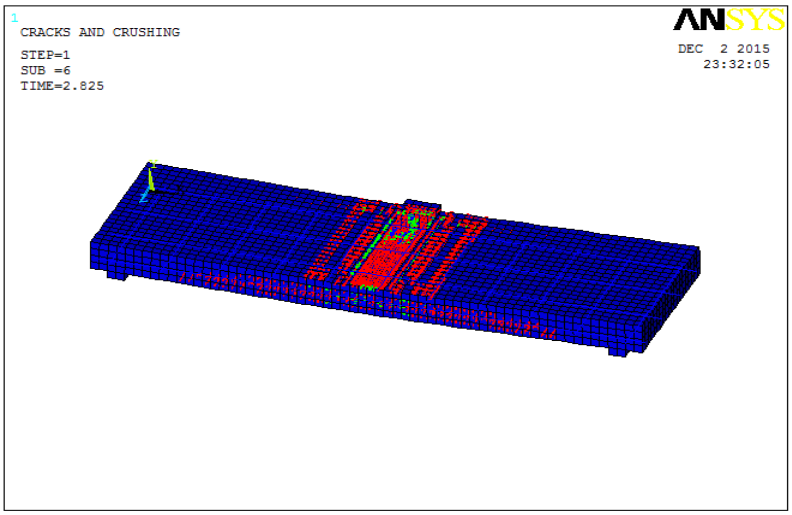

Specimen S-1-1

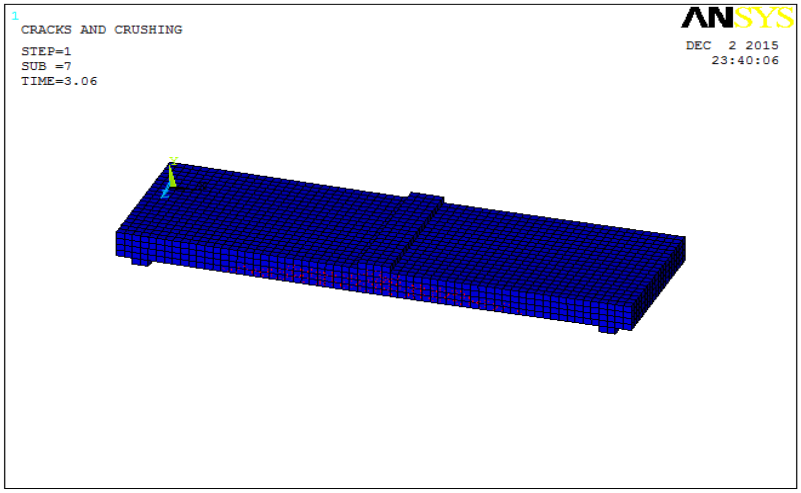

Specimen S-1-2

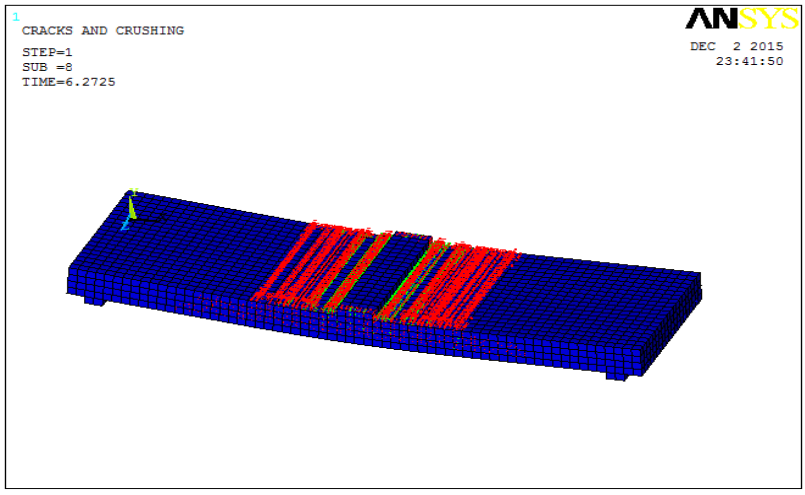

Specimen S-1-3

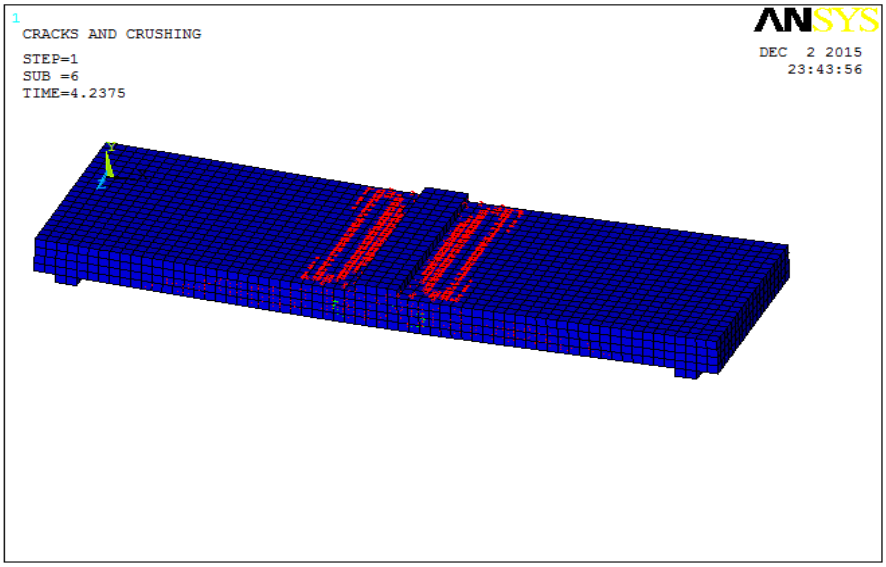

Specimen S-1-4

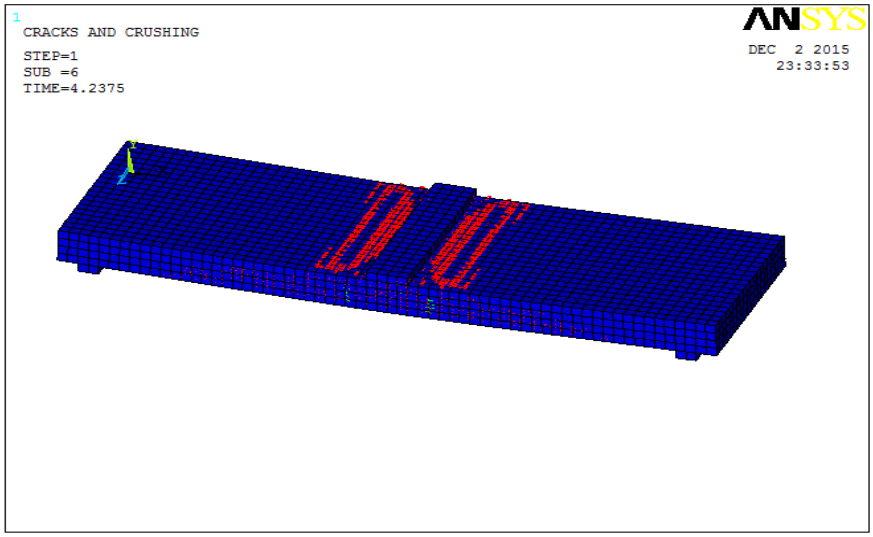

Specimen S-1-5

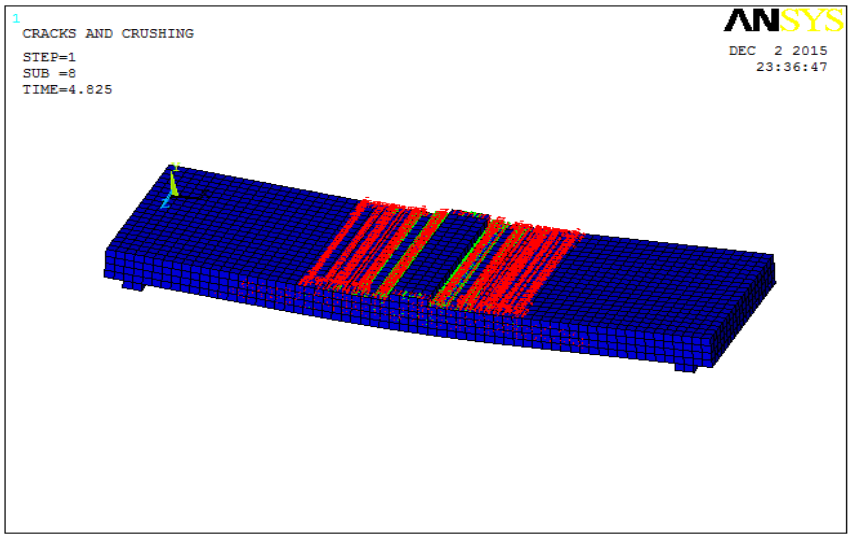

Specimen S-1-6

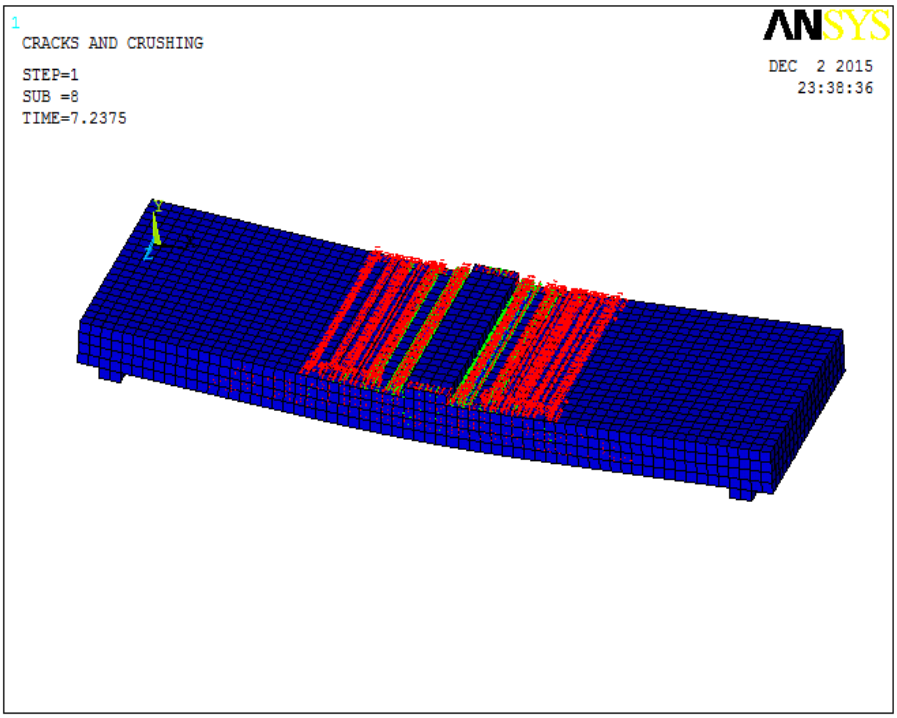

Specimen S-1-7

Fig 16: Crack pattern for group (1)

Figure (17) indicates the effect of reinforcement ratio only for group (1). Effect of reinforcement ratio on failure load for all slabs is nearly the same effect. Slabs (S-1-1,S-1-2,S-1-3,S-1-4 and S-1-5) failed eventually in tension failure after reaching yielding load, Slabs (S-1-6 and S-1-7) failed eventually in compression failure before reaching yielding load, that due to increasing reinforcement area(A_s, A_f) than its maximum value (A_{smax}). Figure (18) and Figure (19) discus the effect of loading type for groups (1, 2 and 7).

From Figure (19), Specimens (S-7-1, S-7-2) increased in their failure load capacity than the specimens (S-1-1, S-1-2, S-2-1 and S-2-2), Specimens which loading by uniform load which distributed on all points have load capacity more than others.

From Figure (19), specimen (S-7-3) there is an increase in its failure load capacity than which for specimens (S-1-3 and S-2-3), which loaded by uniform load. For specimen (S-2-3) failure load increases than value of specimen (S-1-3) have two lines loading. Figure (20) discusses the rectangularity ratio effect on failure load, specimen (S-10-1) increased in their failure load capacity than the specimen (S-6-1), which is loaded by two orthogonal lines load and (S-10-1) loaded by uniform Load all over the area, while, specimen (S-10-2) there is increasing in its failure load capacity than the specimen (S-6-2), which loaded by two orthogonal lines and (S-10-2) which loaded by uniform Load all over the area.

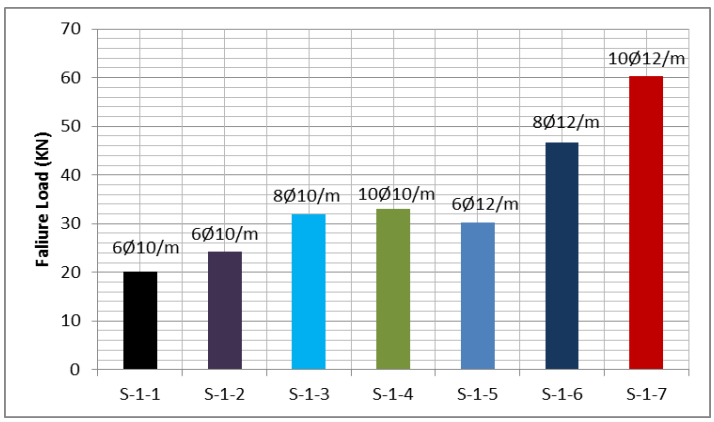

Fig 17: Effect of reinforcement ratio on the failure load

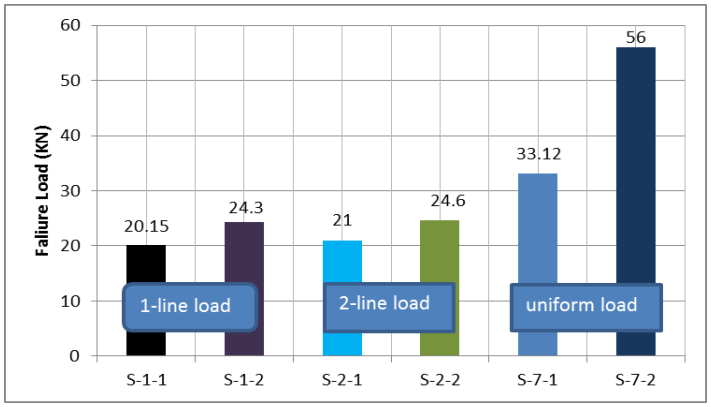

Fig 18: Effect of loading type on the failure load

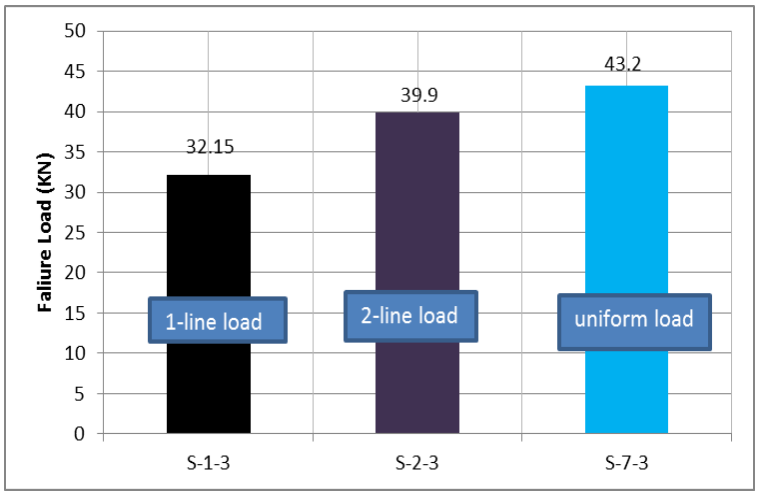

Fig 19: Effect of loading type on the failure load

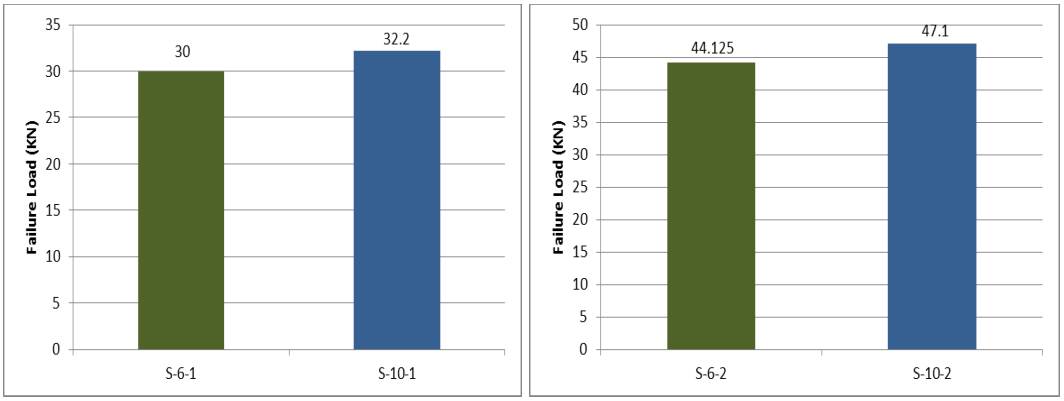

Fig 20: Effect of slab rectangularity ratio on the failure load

4. CONCLUSION

According to the results obtained from this research, the following conclusions can be drawn:

1- Load deflection plot of concrete slabs reinforced using GFRP bars was linear up to cracking stage, followed by an approximately linear part with lower stiffness failure in most curves which is same as those for slabs reinforced using steel bars.

2- Slabs with lower reinforcement ratio ($\mu < 0.9\%$) showed a lower failure load compared by slabs with reinforcement which have ($\mu > 1.1\%$).

3- Slabs with reinforcement ratio ($\mu < 0.9\%$) failed as tension failure but the slabs with reinforcement which ($\mu > 1.1\%$) failed as compression failure.

4- Slabs subjected to uniform load showed a better behaviour than that subjected to concentrated loads regarding to cracks distribution, mode of failure and deflection.

5- The stiffness of slab reinforced using GFRP bars was significantly lower than that reinforced using steel bars with the constant area of reinforcement after cracking, consequently, larger cracks and deflection.

6- Increasing reinforcement ratio of GFRP from 0.55% to 1.3% the stiffness was still lower than which for steel control specimen, that is due to the difference between the elastic modulus of steel and GFRP which is too high to be overcome by increasing the area of reinforcement.

7- Smaller GFRP bars diameter with same reinforcement ratio specimens showed larger difference in failure load and little difference in deflection, the reason is due to the increase of the bond strength between concrete and GFRP bars.

8- Slabs reinforced using GFRP bars achieved higher load capacity than which specimen reinforced using steel bars with constant reinforcement due to higher tensile strength of GFRP bars.

REFERENCES

[1] AbdElnaby, S.F. (1998), "State of the art report on the Use of fiber reinforced Polymers for reinforcing concrete elements" State of the Art Report, Faculty of Engineering, Helwan University, September 1990, p.34

[2] Benmokrane B., Chaallalt O. And Masmoudi R., (2005) "Glass Fiber Reinforced Plastic (GFRP) Rebars for Concrete Structures" Construction and Building Materials, Vol. 9, No. 6, pp. 353-364.

[3] American Concrete Institute (ACI) State-of-the-Art Report (1999),"Provisional Designing Recommendations for Concrete Reinforced with FRP Rebar's "Draft document.

[4] Abdallah, H., El-Badry, M, and Riskalla, S.(1996),"Behaviour of concrete slabs Reinforced by GFRP", Advanced Composite Materials, State-of-the-Art Report, The First Middle East Workshop on the Structural Composite, Ain Shams University by The Egyptian Society of Engineers. Sharm El-Sheikh. Egypt. June 1996, PP. 229-226.

[5] Bedard, Claude (1992), "Composite Reinforcing Bars: Assessing Their Use in Construction" Concrete International, Vo1.14, no.1, pp.55-59.

[6] Alkhrdaji, T., L. Ombres and A. Nanni, (2000) “Flexural Behaviour and Design of One-Way Concrete Slabs Reinforced with Deformed GFRP Bars,” Proc., 3rd Inter. Conf. on Advanced Composite Materials in Bridges and Structures, Ottawa, Canada, J. Humar and A.G. Razaqpur, Editors, pp. 217-224.

[7] American Concrete Institute (ACI) State-of-the-Art Report (2006)."Fiber Reinforced plastic (FRP) Reinforced for Concrete Structures, Report by ACI Committee.440.

[8] Deitz. D. H, HarikI. E, and Gesund. H, (1999)"One-Way Slabs Reinforced with Glass Fiber Reinforced Polymer Reinforcing Bars" Special Publication Volume: 188, P 279-286

[9] Hosny. A.H.H El-Nawawy, O.A. Mostafa. El. And Khalil, A.H.H (1996), ' Behaviour of Concrete Slabs Reinforced with Fiber – Glass Bars '. The 1st Middle East Workshop on Structural Composite, Sharm El-Sheikh, Egypt, PP.

[10] Luciano Ombres, Tarek Alkhrdaji, Antonio Nanni (2000) "Flexural analysis of one way concrete slabs reinforced with GFRP rebars" International meeting on composite materials, PLAST, P 243-250.

[11] Dulude.C, Ahmed. F, El-Gamal.S, (2010) "Testing of Large Scale Two Way Slabs Reinforced with GFRP bars" The 5th international conference on FRP composite in civil Engineering, pp.287.

[12] Haggag, H.A., Hanna, N.F., and Gad, R.M.(2005), "Behaviour of Concrete Slab Reinforced by Both GFRP Rebars and Polypropylene Fibers", Engineering Research Journal, Helwan University, Faculty of Engineering, Mataria, Engineering Research Journal Vol. 126, February 2005, pp85 –95.

[13] Haggag, H.A., Hanna, N.F., and Gad, R.M.(2003), "Behaviour of One-Way Concrete Slab Reinforced by GFRP Rebars and polypropylene Fibers", Engineering Research Journal, Helwan University, Faculty of Engineering, Mataria, Vol. 85, February 2003, pp. 59-67.

[14] ANSYS, "ANSYS Help", Release 14.5, Copyright 2012.

[15] Egyptian Code of Practice (ECCS203-2012) (2012), "Egyptian code for Designing and Constructing Reinforced Concrete Structures", Institute for Building Research, Egypt.

[16] Benmokrane, B.,Tighiouart B., Chaallal O., (1996) "Bond strength and load distribution of composite FRP rebars in concrete" ACI Mater. J.1996;96(3):246-53.

[17] Consenza, E, Manfredi, G., and Realfonzo, R. (1997)," Behaviour and Modeling of Bond of FRP- Rebars to Concrete ", Journal of Composites for Construction, Vol .1, no. 2,pp. 40-51.

[18] A. Abdel-Fattah, M. Said and A. Salah, (2016), "Nonlinear Finite Element Analysis For Reinforced Concrete Slabs Under Punching Loads", International Journal of Civil Engineering and Technology (IJCIET) Volume 7, Issue 3, May –June 2016, pp. 392 –397, Article ID: IJCIET_07_03_040

[19] Piotr Smarzewski, (2015), "Numerical solution of reinforced concrete beam using Newton-Raphson method with adaptive descent", Biuletyn WAT Vol. LXIV, Nr 4, 2015, Lublin University of Technology, Faculty of Civil Engineering and Architecture.